Journal of Marine Science and Application (2019) 18:239–245
https://doi.org/10.1007/s11804-019-00092-8

RESEARCH ARTICLE

Galvanic Interactions of 15CDV6/MDN138 & 15CDV6/MDN250 Alloys in Natural Seawater

P. Ramakrishna rao[1] · G. T. Parthiban[2] · G. Subramanian[3] · K. Muthuraman[2]

Received: 30 January 2017 / Accepted: 18 January 2018 / Published online: 24 June 2019

Abstract

The galvanic corrosion behavior of the metal combinations 15CDV6/MDN138 and 15CDV6/MDN250, with 1:1 area ratio, has been studied in natural seawater using the open well facility of CECRI's Offshore Platform at Tuticorin for a year. The open circuit potentials of MDN138, MDN250, and 15CDV6 of the individual metal, the galvanic potential and galvanic current of the couples 15CDV6/MDN138 and 15CDV6/MDN250, were periodically monitored throughout the study period. The calcareous deposits on MDN138 and MDN250 in galvanic contact with 15CDV6 were analyzed using XRD. The electrochemical behavior of MDN138, MDN250, and 15CDV6 in seawater was studied using an electrochemical work station. The surface characteristics of MDN138 and MDN250 in galvanic contact with 15CDV6 have been examined with a scanning electron microscope. The results of the study reveal that the galvanic protection offered by 15CDV6 to MDN250 and MDN138 in natural seawater amounts to 93% and 98%, respectively, implying that the galvanic protection offered by 15CDV6 is continuous and effective, which has been further evinced from the adherent nature of the calcareous deposit film comprising compounds such as $CaCO_3$ (calcite, aragonite, and vaterite), $MgCO_3$ (magnesite), $Mg(OH)_2$ (brucite), and MgO (brucite).

Keywords MDN138 · MDN250 · 15CDV6 · Galvanic corrosion · Natural seawater

Article Highlights
- The galvanic corrosion behavior of the metal combinations 15CDV6/MDN138 and 15CDV6/MDN250, with 1:1 area ratio, has been studied in natural seawater.
- The galvanic protection offered by 15CDV6 to MDN250 and MDN138 in natural seawater amounts to 93% and 98%, respectively.
- The adherent nature of the calcareous deposit film comprising compounds such as $CaCO_3$ (calcite, aragonite, and vaterite), $MgCO_3$ (magnesite), $Mg(OH)_2$ (brucite), and MgO (brucite), also favors the extent of galvanic protection.
- Electrochemical polarization study reveals that MDN138 alloy is more corrosion resistant than MDN250 alloy.

✉ G. Subramanian
cgscorr@yahoo.co.in

[1] Defence Research Development Laboratory, Hyderabad 500 058, India

[2] CSIR-Central Electrochemical Research Institute, Karaikudi 630 003, India

[3] Corrosion Testing Centre, CSIR-CECRI Unit, , Mandapam Camp 623 519, India

1 Introduction

MDN250 is an 18% nickel, cobalt strengthened steel (C-type), with excellent mechanical properties, workability, and heat treatment characteristics. It is weldable without preheat, in both the annealed and aged condition. The alloy is very tough, relatively soft (30/34 R_c), therefore, readily machined and formed. Typical applications for maraging include missile and rocket motor cases, landing and takeoff gear, munitions, aerospace, extrusion tooling, die casting, high-performance shafting, gears, and fasteners. MDN138 is a precipitation, age-hardenable stainless steel. Its principal features are high transverse toughness, good resistance to general and stress corrosion cracking, and high strength that is developed by a single low-temperature heat treatment and best welded in the solution-annealed condition (Liu 2015). This alloy has been used in aircraft components such as landing gear and structural sections, valves, shafts, and components in the petrochemical and nuclear industries. Alloy 15CDV6 is a low carbon steel which combines a high yield strength (superior to SAE 4130) with good toughness and weld ability. 15CDV6 can be

readily welded with very little loss of properties during welding and without the need for further heat treatment. This alloy finds many applications in the aerospace and motorsports industries in such components as roll cages, pressure vessels, suspensions, rocket motor casings, wish bones, and sub frames. The effect of porosity and slag inclusion on the fatigue fracture behavior of 15CDV6 butt welds has been investigated by Ray et al. (1986). The role of additives for sacrificial protection of steel by aluminum and zinc pigments in model high-temperature coatings has been studied by Serdechnova (2013). Sapthagiri et al. (2015) have investigated the mechanical properties on 15CDV6 steel plates by TIG—welding with and without copper-coated filler wires. In the present study, the galvanic corrosion behavior of the metal combinations 15CDV6/MDN138 and 15CDV6/MDN250, with 1:1 area ratio, has been studied in natural seawater using the open well facility of CECRI's Offshore Platform at Tuticorin for a year, which is first of its kind in the literature of Indian waters.

2 Materials and Methods

2.1 Materials

The materials (15CDV6, MDN138, & MDN250) were supplied by Defence Research and Development Laboratory, Hyderabad. The composition of 15CDV6 is C: 0.14, Si: 0.20, Mn: 1.00, S: 0.015, P: 0.020, Cr: 1.30, Mo: 0.85, V: 0.25 and Fe: Balance. The composition of MDN138 is Al: 1.0%, C: 0.04%, Cr: 12.5%, Mn: 0.18%, Mo: 2.0%, Ni: 7.5%, N: 0.01%, P: 0.01%, Si: 0.1%, S: 0.007%, and Fe: balance. The composition of MDN 250 is Al: 0.07%, C: 0.03%, Cr: 0.5%, Mn: 0.10%, Mo: 4.6%, Ti: 0.3%, Ni: 17.5%, Co: 7.5%, Cu: 0.5%, P: 0.01%, Si: 0.1%, S: 0.008%, and Fe: balance.

2.2 Specimen Preparation and Galvanic Interaction Study by Natural Seawater Exposure

The coupons of 15CDV6, MDN250, & MDN138 of size 75 mm × 50 mm × 6 mm were cut from the respective sheets, removed corrosion products using the recommended pickling solutions (ASTM standards 2017), mechanically polished with different grits silicon carbide metallurgical paper (180, 220, 400, and 600), cleaned, and degreased with acetone and weighed to an accuracy of 10^{-4} g, and stored in desiccators until use. Galvanic contact between the coupons 15CDV6 & MDN250 and 15CDV6 & MDN138 was affected by PVC-sheathed 320SWG copper wires and the contact points were sealed using marine epoxy to prevent crevice corrosion. The galvanically coupled coupons 15CDV6 & MDN250 and 15CDV6 & MDN 138 with 1:1 area ratio were fixed on a wooden frame with grooving and immersed in the natural seawater at a water depth 2 m below the mean low tide level using the open well facility of CECRI's Offshore Platform at Tuticorin. Periodic monitoring of the open circuit potential (OCP) of the coupons 15CDV6, MDN250, & MDN138 and the mixed potentials of the galvanic couples 15CDV6/MDN250 and 15CDV6/MDN138 were made daily using a high impedance voltmeter (Tektronix, Model DMM155) with a saturated calomel electrode. The galvanic current of the couples 15CDV6/MDN250 and 15CDV6/MDN138 was monitored periodically using zero impedance ammeter. The field studies were terminated after 330 days and the digital images of the galvanically coupled coupons, 15CDV6 & MDN138 and 15CDV6 & MDN250, were recorded, with biomass and corrosion products and after removing biomass and corrosion products. The gravimetric corrosion rates of 15CDV6, MDN138, & MDN250 were calculated after removal of corrosion products using the recommended pickling solutions (ASTM standards 2017). The fouling organisms on the surfaces of the galvanically coupled coupons (15CDV6 & MDN138 and 15CDV6 & MDN250) were recorded and visual observations were made on the surfaces of coupons after removal of biomass and corrosion products. The extent of galvanic protection offered by 15CDV6 to MDN138 & MDN250 has been calculated from the gravimetric corrosion rate values of both freely corroded and galvanically coupled MDN138, MDN250, & 15CDV6.

2.3 Physicochemical Characteristics of Seawater

Subsurface seawater was collected from the test location on a quarterly basis during the 12-month study period using a Hydro-Bios (Kiel) water sampler. Analyses were carried out following the standard procedures outlined by Strickland and Parsons (1972) which included general physicochemical parameters, dissolved nutrients, and major ions. Heavy metals in the water samples were extracted following APDC-MIBK pre-concentration procedure (Brooks et al. 1967) and estimated on an atomic absorption spectrometer (GBC 932 Plus).

2.4 Characterization of Calcareous Deposits on MDN138 & MDN250

The galvanic coupled coupons of MDN138 & MDN250 after retrieval from seawater were washed with double distilled water and dried. The calcareous deposits on MDN138 & MDN250 were analyzed using XRD (X'pert PRO PAN analytical diffractometer with Syn master 793^{s}, Netherlands).

2.5 Surface Characterization of MDN138 & MDN250

The fouling assemblage on the galvanic coupled coupons of MDN138 & MDN250 after retrieval from seawater was

scraped and the corrosion products were removed using the recommended pickling solutions (ASTM standards 2017), washed in distilled water, and dried. The surface morphology of the coupons was examined under the scanning electron microscope (SEM) (HITACHI Model S-3000H instruments).

2.6 Electrochemical Behavior of 15CDV6, MDN250, & MDN138 in Natural Seawater

The potentiodynamic polarization curves of 15CDV6, MDN138, & MDN250 were drawn by conducting experiments separately for 15CDV6, MDN138, and MDN250, using AUTOLAB PGSTAT30 in the feed potential range of − 1000 mV to 1000 mV with a 3-electrode cell arrangement with 15CDV6/MDN138/MDN250 as working electrode, Ag/AgCl as reference electrode, and platinum as counter electrode in natural seawater.

3 Results and Discussion

The mean values of physicochemical parameters of seawater of Open sea–Tuticorin are presented in Table 1. In general, the values of the water quality parameters were found to be normal, and did not show much seasonal variation during the study period. Hence, the mean values of the four quarters are taken into consideration. Figure 1 portrays the open-circuit potential values of 15CDV6, MDN250, & MDN138 and galvanic potential values of 15CDV6 & MDN138 and 15CDV6 & MDN250 in natural seawater, recorded throughout the study period. The galvanic current values of the galvanic couples 15CDV6/MDN250 and 15CDV6/MDN138, recorded throughout the study period, are given in Fig. 2.

Table 1 Seawater quality parameters of the Open sea–Tuticorin showing the mean values ($n = 4$) and their SDs

Parameters	Open sea–Tuticorin	
	Mean	Standard deviation
Salinity/‰	35.00	0.74
pH	8.1	0.113389
Dissolved oxygen/(ml·L^{-1})	4.85	0.265922
Inorganic phosphate/(μmol·L^{-1})	0.725	0.074066
Total phosphorous/(μmol·L^{-1})	3.27	1.195894
Nitrite/(μmol·L^{-1})	0.017	0.000983
Nitrate/(μmol·L^{-1})	4.37	0.297
Silicate/(μmol·L^{-1})	18.83	2.76
Ammonia/(μmol·L^{-1})	2.25	0.134164
Calcium/(μg·L^{-1})	400	19.8206
Magnesium/(μg·L^{-1})	1275	97.24784
Copper/(μg·L^{-1})	2.7	0.47
Cadmium/(μg·L^{-1})	1.30	0.217
Lead/(μg·L^{-1})	14	0.7278
Iron/(μg·L^{-1})	54.0	15.928
Manganese/(μg·L^{-1})	5.50	0.790569
Zinc/(μg·L^{-1})	1.570	0.5947
Mercury/(μg·L^{-1})	1.196	0.234379

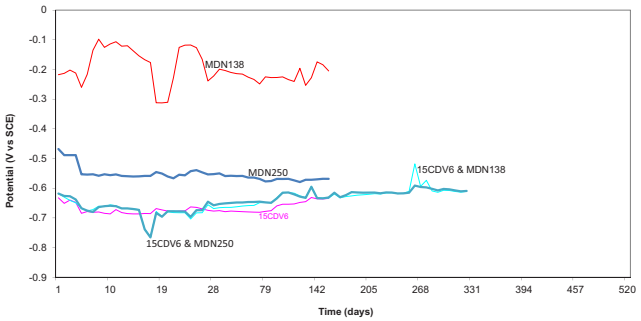

Fig. 1 Open-circuit potential values of 15CDV6, MDN250, & MDN138 and galvanic potential values of 15CDV6 & MDN138 and 15CDV6 & MDN250 in natural seawater

3.1 Visual Observations

3.1.1 15CDV6/MDN250

Figure 3 portrays the digital images of the surface of galvanically coupled 15CDV6 & MDN250 after termination of the experiment. The surface of the galvanically coupled 15CDV6 is characterized by barnacles, oysters, and algae along with reddish orange corrosion products, while that of MDN250 is characterized predominantly by barnacles and oysters and dense algae fouling. Figure 4 portrays the digital images of the surface of galvanically coupled 15CDV6 & MDN250 after removal of corrosion products and biomass. The surface of the galvanically coupled 15CDV6 after removal of corrosion products and biomass is characterized by numerous pits beneath, whereas no characteristic pitting was observed on

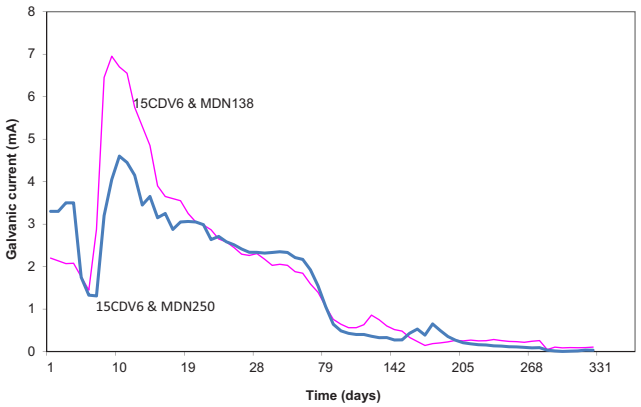

Fig. 2 Galvanic current values of 15CDV6 & MDN138 and 15CDV6 & MDN250 in natural seawater

Fig. 3 Surface of the galvanically coupled coupons of 15CDV6 (left) & MDN250 (right) exposed in natural seawater

MDN250, other than mild etchings beneath the attachment of hard foulers such as barnacle and oysters.

3.1.2 15CDV6/MDN138

Figure 5 portrays the digital images of the surface of galvanically coupled 15CDV6 & MDN138 after termination of the experiment. The surface of the galvanically coupled 15CDV6 is characterized by barnacles and oysters along with reddish orange corrosion products, while that of MDN138 is characterized by barnacles and oysters. Figure 6 portrays the digital images of the surface of galvanically coupled 15CDV6 & MDN138 after removal of corrosion products and biomass. The surface of the galvanically coupled 15CDV6 after removal of corrosion products and biomass is characterized by numerous pits and layering type of corrosion, whereas no characteristic pitting was observed on MDN138.

3.2 Characterization of Calcareous Deposits on MDN138 & MDN250

The nature of calcareous deposits formed on the galvanically protected MDN250 & MDN138 as analyzed by XRD is found to be same and given in Fig. 7. The compounds were identified as $CaCO_3$ (calcite, aragonite, and vaterite), $MgCO_3$ (magnesite), $Mg(OH)_2$ (brucite), and MgO (brucite). With particular reference to $CaCO_3$, more aragonite phases were recorded than calcite or vaterite.

Fig. 4 Surface of the galvanically coupled coupons of 15CDV6 (top) & MDN250 (bottom) after removal of biomass and corrosion products

3.3 Open Circuit Potential, Galvanic Potential, and Galvanic Current

3.3.1 15CDV6/MDN250

The open circuit potentials (OCPs) of 15CDV6 & MDN250, and the galvanic potential of the couple 15CDV6/MDN250, are presented in Fig. 1 At the commencement of the experiment the OCP of 15CDV6 was − 0.6325 V, over the period of exposure it experienced an upward surge at −0.631 V and a downward surge at − 0.6845 V, and at the termination of the experiment the OCP was found to be − 0.634 V.

The OCP of MDN250 from the commencement (− 0.468 V) of the experiment experienced only minor fluctuations (− 0.553 to − 0.568 V) throughout the study period. Over the period of exposure, it experienced a downward surge at − 0.5665 V, and at the termination of the experiment the OCP was found to be − 0.568 V.

The galvanic potential of the couple (15CDV6/MDN250) at the commencement of the experiment was − 0.618 V, over the period of exposure it experienced an upward surge at − 0.5107 V and a downward surge at − 0.7655 V, and at the termination of the experiment it was found to be − 0.609 V. The mixed potential values lie within the OCP values of 15CDV6 throughout the study period. Hence, it is evident that 15CDV6 would have offered protection to MDN250 (Subramanian et al. 2016; Parthiban et al. 2017).

The galvanic current values of the couple 15CDV6/MDN250 over the period of exposure are presented in Fig. 2. The galvanic current of the couple experienced a steep decrease from 4th day (3.5 mA) to 6th day (1.328 mA), from 7th day (1.31 mA) to 10th day (4.6 mA) a steep increase has been observed, and from 11th day (4.45 mA) to 51st day (2.21 mA) a gradual decline has been observed. A drastic reduction from 58th day (2.169 mA) to 142nd day (0.273 mA) has been noticed. The surge in the galvanic

Fig. 5 Surface of the galvanically coupled coupons of 15CDV6 (left) & MDN138 (right) exposed in natural seawater

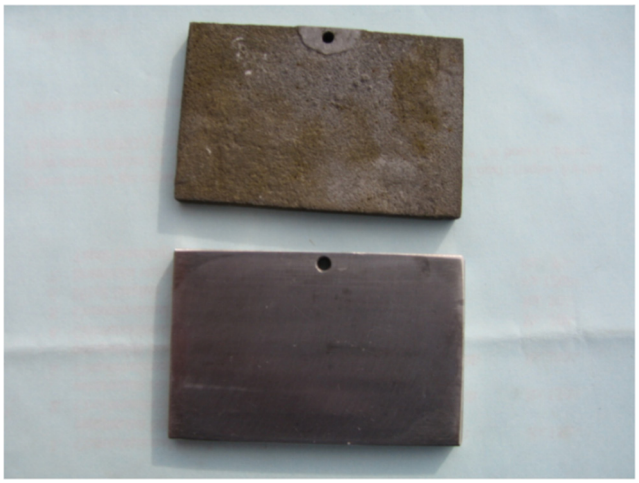

Fig. 6 Surface of the galvanically coupled coupons of 15CDV6 (top) & MDN138 (bottom) after removal of biomass and corrosion products

current values from 7th day to 10th day could be attributed to the initial current demand for effective protection of the cathode surface until the formation of an adherent thin film of calcareous deposit. Cathodic protection alters the ionic concentration at the interface, increasing the hydroxyl ion concentration (Sarlak et al. 2009; Wieng et al. 2007; Parthiban et al. 2017).

A steady state has been attained between 282 (0.832 mA) and 324th day (0.032 mA). Thus, the onset of steady state current has been postponed to the tail end of the experiment (282–324 days); which can be accounted owing to the impairment caused to the calcareous deposit film, by the concomitant effect of turbulence in the sea and settlement of fouling organisms on the cathodic surface (MDN250).

The interrelationships between bacteria and calcareous deposits are not understood thoroughly (Brenda Little and Wagner 1993; Parthiban et al. 2017). The interaction of the biofilm and calcareous deposits on cathodically protected surfaces would result in the dissolution of the deposits by the bacterial secretion and porous deposits could affect the performance of the cathodic protection system (Parthiban et al. 2017). The pattern of the curve infers that 15CDV6 would have offered required amount of protection to MDN250. This has been further supported by the digital image of the surface of the coupon MDN250 and visual observation after removal of biomass and corrosion products.

3.3.2 15CDV6/MDN138

The OCPs of 15CDV6 & MDN138, and the galvanic potential of the couple 15CDV6/MDN138, are presented in Fig. 1. At the commencement of the experiment, the OCP of 15CDV6 was − 0.6325 V, over the period of exposure it experienced an upward surge at − 0.631 V and a downward surge at − 0.6845 V, and at the termination of the experiment the OCP was found to be − 0.634 V.

At the commencement of the experiment, the OCP of MDN138 was − 0.2175 V, over the period of exposure it experienced an upward surge at − 0.098 V and a downward surge at − 0.3105 V, which are more pronounced up to 28th day, and at the termination of the experiment the OCP was found to be − 0.20467 V.

The galvanic potential of the couple (15CDV6/MDN138) at the commencement of the experiment was − 0.618 V, over the period of exposure it experienced an upward surge at − 0.518 V and a downward surge at − 0.764 V, and at the termination of the experiment it was found to be − 0.61067 V. The mixed potential values lie within the OCP values of 15CDV6 throughout the study period. Hence, it is evident that 15CDV6 would have offered protection to MDN138 (Subramanian et al. 2016; Parthiban et al. 2017).

The chemical composition and structure of the calcareous deposit greatly influence the effectiveness of CP. The parameters, such as flow velocity, the calcium and magnesium content of seawater, temperature, dissolved organic matter and

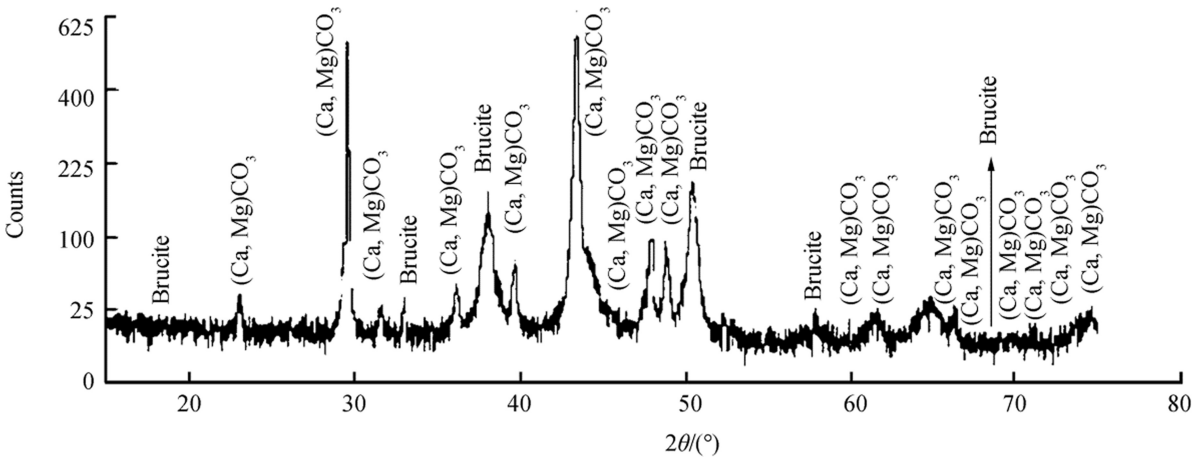

Fig. 7 XRD pattern of calcareous deposits formed on the surfaces of galvanically protected MDN250 & MDN138

pressure, play a key role in deciding the nature of the calcareous deposit. However, interfacial pH is the most significant factor in influencing the deposition kinetics, along with the nature and the stability of the scale (Parthiban et al. 2017).

The galvanic current values of the couple 15CDV6/MDN138 over the period of exposure are presented in Fig. 2. The galvanic current of the couple from the commencement (2.199 mA) experienced a slight decline up to 6th day (1.446 mA), thereafter a steep increase was observed up to 9th day (6.95 mA); and a gradual decline has been observed from 10th day (6.7 mA) to 163rd day (0.237 mA). A near steady state has been observed between 184th day (0.204 mA) and 261st day (0.218 mA); and steady state has been observed between 289th (0.104 mA) and 324th days (0.104 mA). Hence, 15CDV6 would have offered reasonable protection to MDN138. The pattern of the curve infers that 15CDV6 would have offered complete protection to MDN138 during the entire study period (Subramanian et al. 2016; Parthiban et al. 2017).

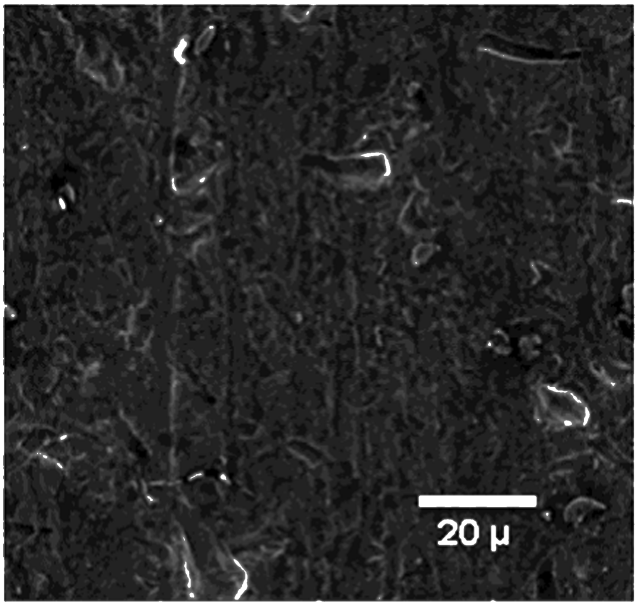

(a) MDN138

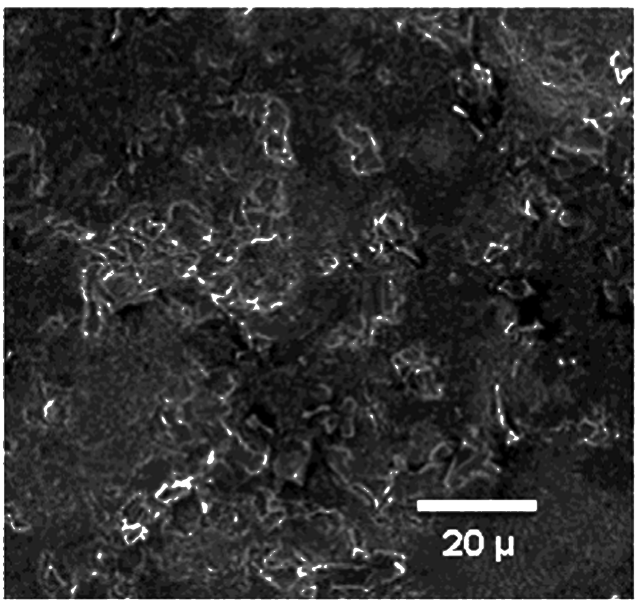

(b) MDN250

Fig. 8 Surface morphology of the galvanically protected. **a** MDN138 and **b** MDN250

3.3.3 Extent of Galvanic Protection Offered by 15CDV6 to MDN250 & MDN138

The numerous undulations in the galvanic current curve of the 15CDV6/MDN138 reveal that 15CDV6 would have experienced more dissolution in order to offer protection to MDN138. Unlike 15CDV6 of 15CDV6/MDN138 couple, the 15CDV6 of 15CDV6/MDN250 would have experienced less dissolution in order to offer complete protection to MDN250, in view of the less potential difference between 15CDV6 & MDN250 and also the lesser undulations in the galvanic current curve of the couple 15CDV6/MDN250. The galvanic protection offered by 15CDV6 to MDN250 and MDN138 during the study period of 330 days amounts to 93% and 98%, respectively. According to the recent study by Yang et al. (2015), the calcareous deposits formed owing to cathodic protection comprised of two layers, inner magnesium rich layer and the outer calcium rich layer. The layers have a clear boundary and randomly distributed pores running through the layers filled with magnesium-rich compounds providing sites for reduction-oxidation and associated mass transport. This vindicates the Elbeik et al. (1986) observation that formation of calcareous deposits on steel surface would lead to a five-fold decrease in the corrosion current. Thus, it further reaffirms that the galvanic protection offered by 15CDV6 is continuous and effective, which has been evinced from the adherent nature of the calcareous deposit film comprising compounds such as $CaCO_3$

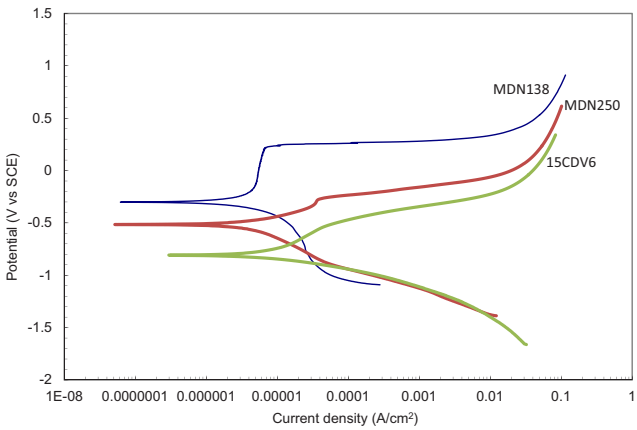

Fig. 9 Potentiodynamic polarization curves of 15CDV6, MDN250, & MDN138 in natural seawater

(calcite, aragonite, and vaterite), $MgCO_3$ (magnesite), $Mg(OH)_2$ (brucite), and MgO (brucite), despite the local disturbances by the combined effect of turbulence in the sea and settlement of fouling organisms on the cathodic surface (Subramanian et al. 2016; Parthiban et al. 2017).

3.4 Surface Characteristics of MDN138 & MDN250 in Galvanic Contact with 15CDV6

Surface morphologies of the galvanically protected MDN138 and MDN250 are portrayed in Fig. 8. The surface morphology of the MDN138 specimen in galvanic contact with 15CDV6 reveals that no characteristic corrosion region could be observed and the whole surface has been covered by the uniform film of calcareous deposits, thus the entire surface has been well protected throughout the study period. Likewise, the surface morphology of the MDN250 specimen in galvanic contact with 15CDV6 reveals that no characteristic corrosion region could be observed and the whole surface has been covered by the uniform film of calcareous deposits, thus the entire surface has been well protected throughout the study period. The signs of minute white spots on the MDN250 would be accounted for the partly unremoved particles of calcareous film even after cleaning in pickling solution.

3.5 Potentiodynamic Polarization Scans of 15CDV6, MDN138, & MDN250

Potentiodynamic polarization curves of 15CDV6, MDN250, & MDN138 in natural seawater are given in Fig. 9. Potentiodynamic polarization scans of freely corroded 15CDV6, MDN138, & MDN250 in natural seawater reveal the characteristic nature of the individual metal and the trend corroborates with open-circuit potential values of the individual metal. The corrosion current values (I_{corr}) are in the order of 15CDV6 > MDN250 > MDN138. Hence, among MDN250 & MDN138, the MDN138 alloy is more corrosion resistant (Liu 2015; Subramanian et al. 2016; Parthiban et al. 2017).

4 Conclusions

The galvanic protection offered by 15CDV6 to MDN250 and MDN138 in natural seawater amounts to 93% and 98%, respectively, revealing that the protection is continuous and effective, which has been further evinced from the adherent nature of the calcareous deposit film comprising compounds such as $CaCO_3$ (calcite, aragonite, and vaterite), $MgCO_3$ (magnesite), $Mg(OH)_2$ (brucite), and MgO (brucite), despite the local disturbances by the combined effect of turbulence in the sea and settlement of fouling organisms on the cathodic surface. The surface morphologies of MDN138 & MDN250 reveal that there is no characteristic corrosion spot implying the extent of protection offered by 15CDV6. Electrochemical polarization study reveals that MDN138 alloy is more corrosion resistant than MDN250 alloy.

Acknowledgements The authors wish to thank the Director, CSIR-Central Electrochemical Research Institute, Karaikudi, for permission and encouragements.

Funding This study has been financially supported by Project Director, DRDL, Hyderabad, India (Project No. SSP 0709).

References

ASTM G1-03(2017)e1. Standard practice for preparing, cleaning, and evaluating corrosion test specimens, ASTM International, West Conshohocken, PA,1–8

Brenda Little J, Wagner PA (1993) The interrelationship between marine biofouling and cathodic protection. Corrosion. NACE. Houston, TX. Paper No. 525

Brooks RR, Presley BJ, Kaplan IR (1967) APDC-MIBK extraction system for the determination of trace elements in saline waters by atomic absorption. Talanta 14:806–816

Elbeik S, Tseung ACC, Mackay AL (1986) The formation of calcareous deposits during the corrosion of mild steel in seawater. Corros Sci 26(9):669–680. https://doi.org/10.1016/0010-938X(86)90032-6

Liu H (2015) Mechanical properties and corrosion behaviors of novel Cr2Ni low-alloy construction steel. Int J Electrochem Sci 10:2130–2140

Parthiban GT, Subramanian G, Muthuraman K, Ramakrishna rao P (2017) Galvanic interactions of HE15/ MDN138 & HE15/MDN 250 alloys in natural seawater. J Mar Sci Appl 16(2):237–242. https://doi.org/10.1007/s11804-017-1412-z

Ray AK, Dwarakadasa ES, Raman KS (1986) Effect of porosity and slag inclusion on the fatigue fracture behaviour of 15CDV6 butt welds. J Mat SciLetters 5:765

Sapthagiri S, Jayathirtha Rao K, Ashok Reddy K, Sharada Prabhakar C (2015) Comparison of mechanical properties on 15CDV6 steel plates by TIG – welding with and without copper coated filler wires. Intl J Adv Res Found 2(5):16–20

Sarlak M, Shahrabi T, Zamanzade M (2009) Investigation of calcareous deposits formation on copper and 316L stainless steel under cathodic polarization in artificial seawater. Protection of Metals and Physical Chemistry of Surfaces 45(2):216–222. https://doi.org/10.1134/S2070205109020166

Serdechnova M (2013) Le controle de reactivite d'auminium en peintue anto-corrosion resistant a la haute temperature. Chimie theorique et/ou physique, Universite Pierre et Marie Curie – Paris VI, 2012. Francais, https://tel.archives-ouvertes.fr/tel-00836639

Strickland JDH, Parsons TR (1972) A practical handbook of seawater analysis, Ottawa (Canada). Fisheries Research Board of Canada 310

Subramanian G, Parthiban GT, Muthuraman K, Ramakrishna rao P (2016) Galvanic corrosion behaviour of HE20/MDN138 & HE20/MDN250 alloys in natural seawater. J Mar Sci Appl 15(3):343–348. https://doi.org/10.1007/s11804-016-1375-5

Yang Y, David SJ, Victorovna KE (2015) A study of calcareous deposits on cathodically protected mild steel in artificial seawater. Metals 5:439–456. https://doi.org/10.3390/met5010439

Wieng SM, Osvoll H, Gartland PO (2007) Efficient cathodic protection to stainless steel small bore tubing. Corrosion. NACE. Houston, TX. Paper No. 07078